Molecular Therapy
Methods & Clinical Development
Original Article

Cell-penetrating peptides enhance the transduction of adeno-associated virus serotype 9 in the central nervous system

Yuan Meng,[1,3] Dong Sun,[2,3] Yiyan Qin,[2] Xiaoyi Dong,[2] Guangzuo Luo,[2] and Ying Liu[1]

[1]Department of Biochemistry and Molecular Biology, China Medical University, Shenyang 110122, China; [2]Institute of Translational Medicine, China Medical University, Shenyang 110122, China

Recombinant adeno-associated viruses (rAAVs) have been widely used in the gene therapy field for decades. However, because of the challenge of effectively delivering rAAV vectors through the blood-brain barrier (BBB), their applications for treatment of central nervous system (CNS) diseases are quite limited. In this study, we found that several cell-penetrating peptides (CPPs) can significantly enhance the *in vitro* transduction efficiency of AAV serotype 9 (AAV9), a promising AAV vector for treatment of CNS diseases, the best of which was the LAH4 peptide. The enhancement of AAV9 transduction by LAH4 relied on binding of the AAV9 capsid to the peptide. Furthermore, we demonstrated that the LAH4 peptide increased the AAV9 transduction in the CNS *in vitro* and *in vivo* after systemic administration. Taken together, our results suggest that CPP peptides can interact directly with AAV9 and increase the ability of this AAV vector to cross the BBB, which further induces higher expression of target genes in the brain. Our study will help to improve the applications of AAV gene delivery vectors for the treatment of CNS diseases.

INTRODUCTION

Recombinant adeno-associated virus (rAAV) vectors have been widely used for preclinical and clinical studies for decades.[1,2] Three AAV vector-based gene therapies (Glybera, Luxturna, and Zolgensma) have already received marketing authorization in the United States and Europe, and several other promising AAV-mediated gene therapy medicines are in phase III clinical trials.[3–6] rAAV vectors are also considered as promising platforms for the treatment of central nervous system (CNS) disorders.[7,8] However, because AAV vectors cannot efficiently cross through the blood-brain barrier (BBB), AAV-mediated gene therapy for CNS diseases has to be reached by either the intraparenchymal injection or the high-dosage system administration.[9] Although intraparenchymal injection can successfully deliver the AAV vectors to a local area of the brain, most neurodegenerative disorders, such as amyotrophic lateral sclerosis, Huntington's disease, leukodystrophies, and lysosomal storage diseases, involve cell damage in multiple areas but not a single site.[10,11] In addition, the side effects of intraparenchymal injection are another concern of this clinical method. To overcome the drawback of intraparenchymal injection, the systemic administration of AAV vectors has been explored to treat CNS diseases.[12,13]

It has been shown that some AAV serotypes, such as AAV7, AAV8, AAV9, AAVrh.8, and AAVrh.10, have demonstrated the ability to transduce neurons and other types of brain cells, the best of which is AAV9.[14–17] AAV9 possesses the remarkable ability to transduce neurons, parenchymal brain cells, and portions of the BBB endothelium. It is considered as a very promising AAV vector for CNS diseases. However, although AAV9 has a higher transduction efficiency in brain than do other AAV serotypes, its transduction efficiency in brain is drastically lower than that in other tissues.[18] To improve the transduction efficiency, the dose of AAV vectors for system administration is much higher than that of local injection.[19,20] The higher dosage usually leads to a higher immune response, which will decrease the efficiency of gene therapy.[21–23] Currently, there are two main methods to improve the AAV transduction efficiency in the brain. The AAV capsid engineering has been used to look for high transduction AAV mutants.[24–27] For example, Deverman et al.[28] generated an AAV9 capsid mutant, AAV-PHP.B, using an evolution approach. This novel AAV serotype contains a 7-aa insertion in the VP1 capsid protein and is distinguished from AAV9 by its high potency to cross the BBB and transduce CNS cells with about 40-fold greater efficiency than AAV9 without significant increases in peripheral organ transduction. Another method is to use cell-penetrating peptides (CPPs) to improve the internalization of AAV capsid into cells through the endocytosis process. CPPs are short peptides, which are able to pass through tissues and cell membranes via energy-dependent or independent mechanisms. CPPs are considered as drug delivery vehicles because they can bind with a wide variety of biologically active conjugates, including proteins, peptides, DNAs, small interfering RNAs (siRNAs), and small

Received 19 November 2020; accepted 23 February 2021;
https://doi.org/10.1016/j.omtm.2021.02.019.

[3]These authors contributed equally

Correspondence: Ying Liu, Department of Biochemistry and Molecular Biology, China Medical University, Shenyang, 110122, China.
E-mail: liuying@cmu.edu.cn
Correspondence: Guangzuo Luo, Institute of Translational Medicine, China Medical University, Shenyang 110122, China.
E-mail: gzluo@cmu.edu.cn

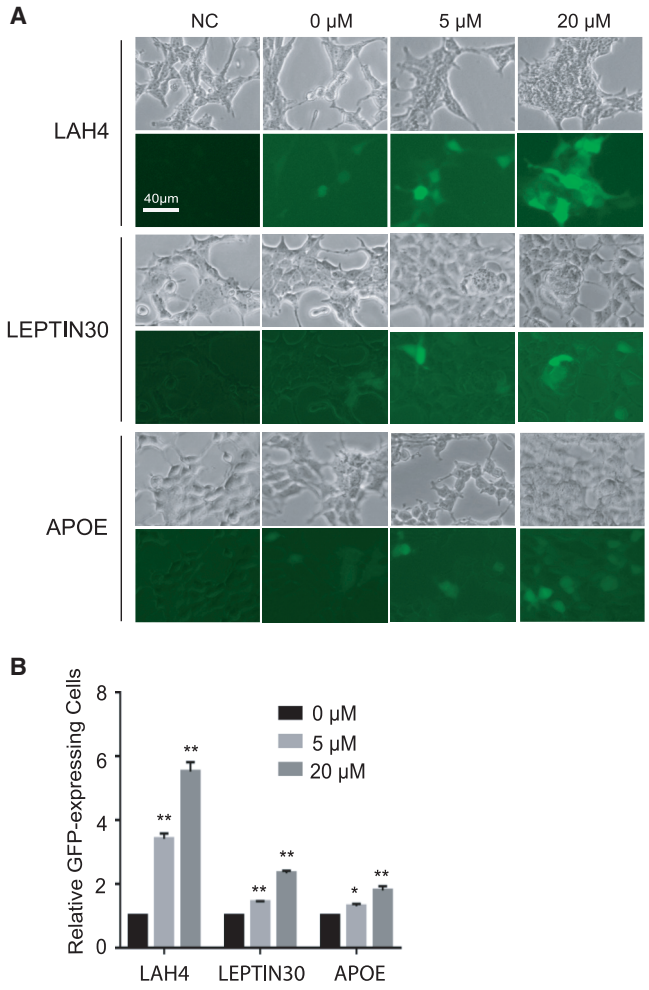

Figure 1. CPPs improve AAV9 transduction in HEK293T cells

(A) Peptides of LAH4, LEPTIN30, and APOE increased AAV9 transduction to HEK293T cells. HEK293T cells were infected with AAV9/GFP (multiplicity of infection (MOI) of 1,000) alone or precomplexed without or with 5 or 20 μM LAH4, LEPTIN30, or APOE. Images were taken by an inverted fluorescence microscope (Nikon). (B) Quantification of green fluorescent protein (GFP) fluorescence level in (A). Error bars represent the standard error of the mean (SEM) from triplicate experiments. Data are means ± SEM (n = 3; >100 cells per experiment). *$p < 0.05$, **$p < 0.01$, by one-way ANOVA followed by a Turkey's test.

drugs, and help these molecules transport into cells.[29] Numerous preclinical studies have been performed to investigate applications of CPP-derived therapeutics, some of which have entered into clinical trials.[30–33] Recently, it was reported that several CPPs can significantly improve the transduction of AAV2 and AAV8 in mouse muscles.[34] Zhang et al.[35] also found that BBB shuttle peptides can significantly enhance AAV8 transduction in the brain and liver *in vivo* after systemic administration.

In this study, we showed that several CPPs, including LAH4, LEPTIN30, and APOE, can significantly enhance the *in vitro* transduction efficiency of AAV9, the best of which was the LAH4 peptide. The enhancement of AAV9 transduction relied on binding of the AAV9 capsid to the peptide. We also demonstrated that the LAH4 peptide increased the AAV9 transduction in the brain and liver after systemic administration. Our results suggest that CPPs can interact directly with AAV9 and increase the ability of this AAV vector to cross the BBB, which further induces higher expression of target genes in the brain.

RESULTS

CPPs enhanced AAV9 transduction in HEK293T cells

It has been reported that CPPs can enhance the transduction of AAV2 and AAV8 *in vivo* and *in vitro*.[34,35] However, whether CPPs can improve transduction of AAV9, the most promising AAV serotype for CNS diseases, is unknown. AAV9 has been speculated to be able to cross through the BBB more efficient than any other AAV serotypes.[9,15] To test the effects of CPPs on the transduction of AAV9, the peptide of LAH4, LEPTIN30, or APOE was incubated with an AAV9 vector encoding green fluorescent protein (GFP) and the transduction efficiency was examined after infection of HEK293T cells. Increasing concentrations of CPPs (0, 5, and 20 μM) were used against fixed amounts of AAV9 (multiplicity of infection [MOI] of 1,000). As shown in Figures 1A and 1B, LAH4, LEPTIN30, and APOE induced a dose-dependent enhancement of viral transduction in HEK293T cells. As expected, there was no fluorescence found in cells without AAV9 transduction (negative control [NC]). In cells incubated with the AAV9 vector only, there was very weak fluorescence in cells. However, the GFP-expressing cells increased about 340%, 140%, and 130% when the AAV9 vector was incubated with peptide (5 μM) of LAH4, LEPTIN30, or APOE and then transduced into HEK293T cells. When the concentration of CPPs increased to 20 μM, the GFP-expressing cells increased about 540%, 230%, and 170% compared to cells transduced with AAV9 only, respectively, the best of which is LAH4. These results indicate that CPPs can efficaciously improve the transduction of AAV9 into human cells.

Enhanced AAV9 transduction mediated by CPPs in endothelial cells (ECs) and human astrocytes (HAs)

Since CPPs are able to enhance AAV9 transduction to HEK293T cells, we wanted to know whether these CPPs can also enhance the transduction of AAV9 into the human brain cells. The BBB is a highly selective permeability barrier that separates the circulating blood from the brain extracellular fluid in the CNS and prevents entry into the brain of most drugs from the blood. The major BBB components include brain microvascular ECs and astrocytes. Brain microvascular ECs help to regulate the flow of substances into and out of the brain, while astrocytes are essential for the formation and integrity of the BBB. Astrocytes are the major type of glial cells in the mammalian brain and provide a variety of supportive functions to their partner neurons in the CNS, such as neuronal guidance during development, and nutritional and metabolic support throughout life.[36–38] To examine the role of CPPs on AAV9 transduction in human cells, the peptide of LAH4, LEPTIN30, or APOE was incubated with an AAV9 vector encoding GFP, and the transduction efficiency was assayed after infection of human cerebral microvascular ECs and HAs.

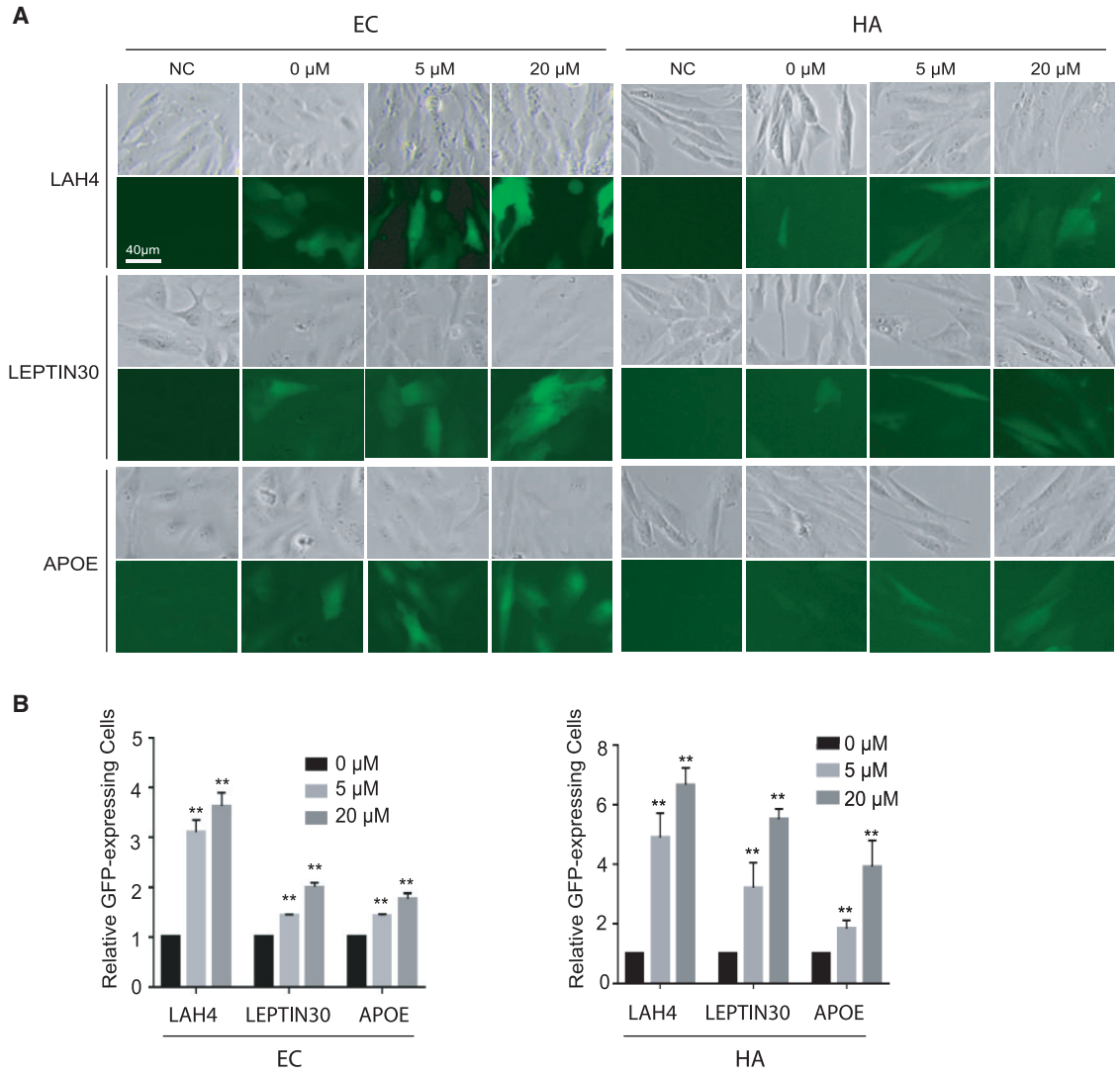

Figure 2. CPPs improve AAV9 transduction in ECs and HAs

(A) Peptides of LAH4, LEPTIN30, and APOE increased AAV9 transduction to ECs and HAs. ECs or HAs were infected with AAV9/GFP (MOI of 1,000) alone or precomplexed without or with 5 or 20 μM LAH4, LEPTIN30, or APOE. Images were taken by an inverted fluorescence microscope (Nikon). (B) Quantification of GFP-expressing cells in (A). Error bars represent the SEM from triplicate experiments. Data are means ± SEM (n = 3; >100 cells per experiment). **p < 0.01, by one-way ANOVA followed by a Turkey's test.

Increasing concentrations of CPPs (0, 5, and 20 μM) were used against fixed amounts of AAV9 (MOI of 1,000). As shown in Figures 2A and 2B, LAH4, LEPTIN30, and APOE induced a dose-dependent enhancement of viral transduction in ECs and HAs, which is similar to that in HEK293T cells. As expected, there was no fluorescence found in cells without AAV9 transduction (NC). In cells incubated with the AAV9 vector only, there was very weak fluorescence in cells. However, the number of GFP-expressing cells significantly increased about 310%, 142%, and 140% in ECs and 490%, 350%, and 220% in HAs when the AAV9 vector was incubated with the peptide (5 μM) of LAH4, LEPTIN30, or APOE and then transduced with ECs or HAs, respectively. Compared to cells transduced with AAV only, when the concentration of CPPs increased to 20 μM, the number of GFP-expressing cells increased about 360%, 200%, and 170% in ECs and 750%, 590%, and 410% in HAs, respectively. Similar to HEK293T cells, LAH4 was the most effective peptide for enhancing viral transduction in ECs and HAs, as compared to that of LEPTIN30 and APOE. Based on these data, we conclude that CPPs can efficiently improve the transduction of AAV9 into ECs and HAs.

CPPs significantly increased the target gene expression delivered by AAV9

Because LAH4, LEPTIN30, and APOE can enhance the AAV9-GFP transduction in HEK293T cells, ECs, and HAs, we speculated that

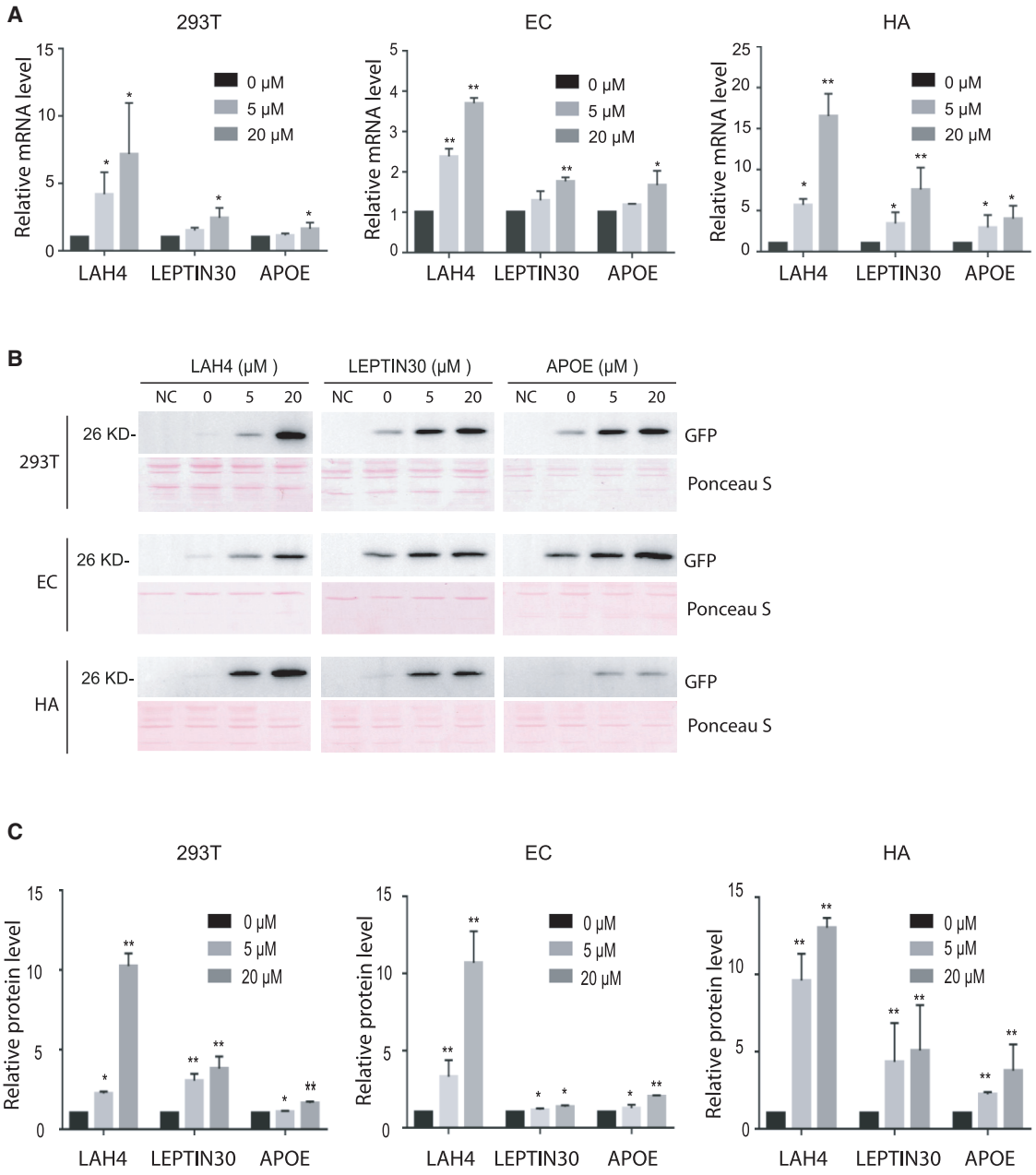

Figure 3. CPPs improve the target gene expression in HEK293T cells, ECs, and HAs

(A) Peptides of LAH4, LEPTIN30, and APOE increased GFP mRNA level in cells. HEK293 cells, ECs, or HAs were infected with AAV9-GFP (MOI of 1,000) alone or pre-complexed without or with 5 or 20 μM LAH4, LEPTIN30, or APOE. Total RNA was isolated from cells, and mRNA levels of GFP were assessed by quantitative polymerase chain reaction (qPCR). The $2^{-\Delta\Delta Ct}$ method was used to calculate the relative GFP mRNA level. All of the data were then normalized by the mean percentage of GFP expression in AAV9 only cell. All error bars represent the SEM from triplicate experiments. Data are means ± SEM (n = 3). *$p < 0.05$, **$p < 0.01$, by one-way ANOVA followed by a Turkey's test. (B) Peptides of LAH4, LEPTIN30, and APOE increased GFP protein level in cells. HEK293 cells, ECs, or HAs were infected with AAV9/GFP (MOI of 1,000) alone or precomplexed without or with 5 or 20 μM LAH4, LEPTIN30, or APOE. Total protein was extracted and GFP expression levels in three cell lines were determined by western blots. Ponceau S-stained total protein was used as a loading control. (C) Quantification of the level of GFP protein in (B). Error bars represent the SEM from triplicate experiments. Data are means ± SEM (n = 3). *$p < 0.05$, **$p < 0.01$, by one-way ANOVA followed by a Turkey's test.

the expression of the GFP gene should also increase accordingly. To test this hypothesis, we purified the total RNA from the cells in Figures 1 and 2 and performed quantitative real-time reverse-transcriptase polymerase chain reactions (RT-PCRs). As shown in Figure 3A, LAH4, LEPTIN30, and APOE induced a dose-dependent increasing of GFP mRNA level in HEK293T cells, ECs, and HAs. In cells

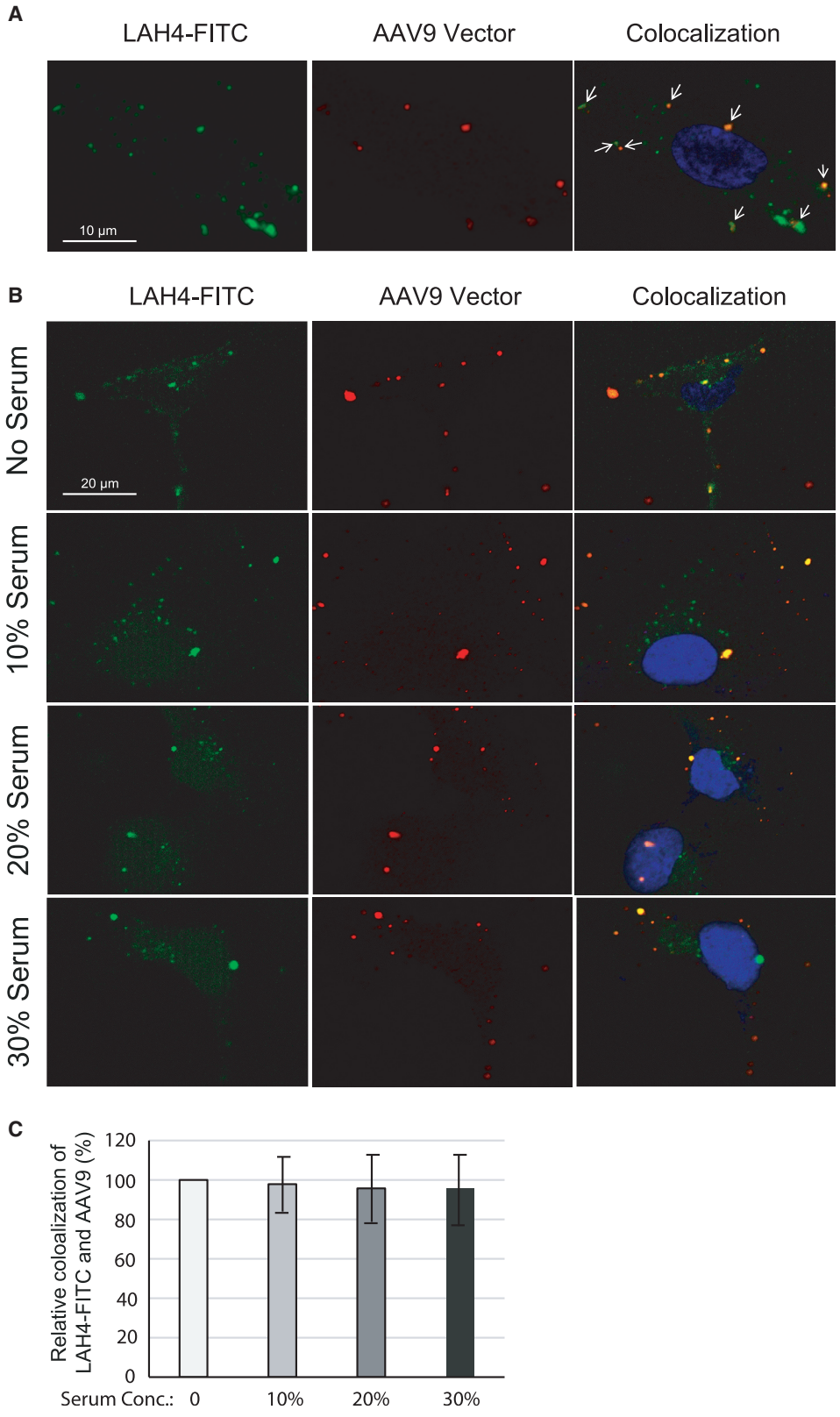

(legend on next page)

incubated with the AAV9 vector only, there was a very low level of GFP mRNA in cells. However, compared to cells transduced with AAV, only the mRNA level significantly increased about 357%, 150%, and 110% in HEK293T cells, 230%, 130%, and 115% in ECs, and 550%, 350%, and 270% in HAs, respectively, when the AAV9 vector was incubated with the peptide (5 μM) of LAH4, LEPTIN30, or APOE and then transduced with HEK293T cells, ECs, or HAs. Compared to cells transduced with AAV only, when the concentration of CPPs increased to 20 μM, the mRNA level increased about 700%, 200%, and 170% in HEK293T cells, 360%, 170%, and 120% in ECs, and 1,600%, 730%, and 445% in HAs, respectively.

We also examined the GFP protein level by immunoblots using mouse anti-GFP antibody. As shown in Figures 3B and 3C, LAH4, LEPTIN30, and APOE induced a dose-dependent increasing of GFP protein level in HEK293T cells, ECs, and HAs. In cells incubated with the AAV9 vector only, there was a very low level of GFP protein in cells. However, when the AAV9 vector was incubated with the peptide (5 μM) of LAH4, LEPTIN30, or APOE and then transduced with HEK293T cells, ECs, or HAs, the protein level increased about 216%, 310%, and 100% in HEK293T cells, 330%, 160%, and 130% in ECs, and 1,000%, 650%, and 220% in HAs compared to cells transduced with AAV vector only, respectively. When the concentration of CPPs increased to 20 μM, the protein level increased about 1,000%, 380%, and 160% in HEK293T cells and 990%, 130%, and 200% in ECs and 1,200%, 700%, and 370% in HAs compared to cells transduced with AAV vector only, respectively.

To characterize the effect of these peptides on the target cells, the viability of cells was determined by an MTT (3-(4,5-dimethylthiazol-2-yl)-2,5-diphenyltetrazolium bromide) assay after incubation with either AAV9-CPP complexes or AAV9 alone. As shown in Figure S1, no cytotoxicity was observed when AAV9 was preincubated with CPPs at concentrations up to 20 μM. Taken together, CPPs, especially LAH4, can significantly enhance the target gene expression in HEK293T cells, ECs, and HAs delivered by AAV9 vector.

Colocalization of the LAH4 peptides and AAV9 vector particles in cells

We next sought to determine whether the enhanced viral transduction mediated by CPPs resulted from a direct interaction of the AAV9 vector particles and CPPs, and whether the mouse serum affects the stability of the AAV9-CPP complex. To test this speculation, empty capsid AAV9 particles without transgene were pre-incubated with 5 μM fluorescein isothiocyanate (FITC)-labeled LAH4 peptides at 37°C for 1 h. The mixture was then incubated with ECs, respectively. After 3 h, the cells were collected and fixed, and images were captured by fluorescence confocal microscopy. AAV9 was immunostained with an antibody specific for intact AAV particles. As shown in Figure 4A, most of the AAV9 vectors were colocalized with FITC-labeled LAH4 peptides, suggesting the formation of AAV9-LAH4 complexes. This result strongly confirmed the speculation that the enhanced viral transduction mediated by CPPs resulted from a direct interaction of AAV9 particles and CPPs. To explore whether the AAV9-LAH4 complex is suitable for administration in mammals, the effect of serum on the stability of the AAV9-LAH4 complex was examined. As shown in Figures 4B and 4C, adding of 10%–30% mouse serum into the incubation reaction of AAV9 and LAH4 did not significantly change the colocalization of LAH4-FITC and AAV9 in the cells, suggesting that the mouse serum did not dissociate the AAV9-LAH4 complex *in vitro*.

Optimization of AAV9-LAH4 complex formation

To optimize the experimental conditions for producing AAV9-CPP complex mixture with the most potent transduction efficiency, we first examined the transduction efficiency of the AAV9-LAH4 complex mixture formed after incubation the 1×10^4 vector genomes (vg) of AAV9 particles encoding GFP and 5 μM LAH4 peptide for 0, 60, and 120 min, respectively. The AAV9-LAH4 complex mixtures were then incubated with ECs for transduction for 24 h. The cells were examined by fluorescence microscopy. As shown in Figure 5A, LAH4 induced a time-dependent increasing of fluorescence level in ECs. Without incubation of AAV9 and LAH4 (time 0), there was very weak fluorescence in cells. The fluorescence level significantly increased when the AAV9 vectors were incubated with the LAH4 peptide for 2 h. We also extracted the total RNA and protein from the cells in Figure 5A and examined the GFP mRNA level and protein level with quantitative real-time RT-PCR and western blot, respectively. As shown in Figures 5B–5D, similar to the fluorescence level, the LAH4 peptide also induced a time-dependent increasing of GFP mRNA and protein level in ECs. After incubation for 2 h, both the GFP mRNA and protein levels were about 350% and 260% higher than those without incubation (time 0).

It has been suggested that CPPs interact with AAV particles through a covalent bond, which is an energy-dependent process, and that the temperature affects formation of the AAV-CPP complex.[32,34] To examine whether formation of the AAV9-CPP complex is also a temperature-dependent process, we examined the transduction efficiency of the AAV9-LAH4 complex formed at 4°C, 25°C, and 37°C, respectively. The AAV9-CPP complex mixtures were incubated with ECs for transduction for 24 h. The cells were then examined by fluorescence microscopy. As shown in Figure 5E, the LAH4 peptide induced a temperature-dependent increase of fluorescence levels in ECs. At

Figure 4. Colocalization of the LAH4 peptides and AAV9 particles in cells

(A) AAV9 particles were incubated with FITC-CPP (green) and subsequently probed with a mouse monoclonal antibody specific for intact AAV (red). The nucleus is in blue and a single cell is shown. Overlapping green and red signals appear as yellow in the merged image. The image was taken by a Nikon confocal microscope. Arrows indicate colocalized AAV9 particles and LAH4 peptides. Scale bar represents 10 μm. (B) The AAV9-LAH4-FITC mixture was incubated without or with mouse serum and subsequently probed with a monoclonal antibody specific for intact AAV (red). Overlapping green and red signals appear as yellow in the merged image. The image was taken by Nikon confocal microscope. Scale bar represents 20 μm. (C) Quantification the colocalization of each cell in (B). n = 3; >50 cells per experiment.

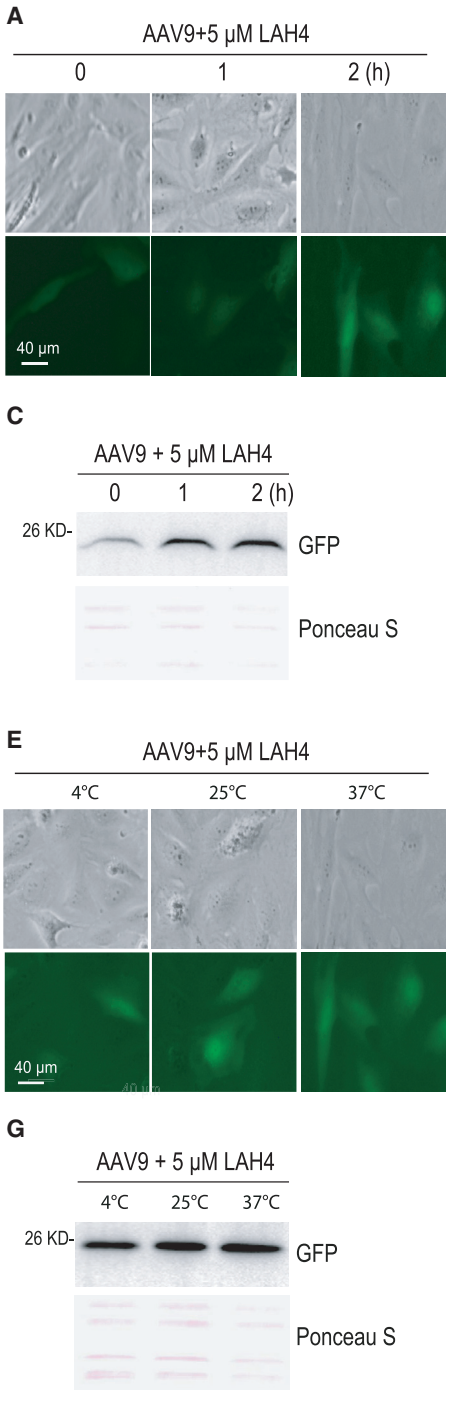

Figure 5. Optimization of AAV9-LAH4 complex formation

(A) Effect of incubation time on AAV9 transduction efficiency. Scale bar represents 40 μm. (B) Total RNA was isolated from cells in (A), and mRNA levels of GFP were assessed by qPCR. Data are means ± SEM (n = 3; one-way ANOVA followed by t test). **p < 0.01. (C) GFP protein level in ECs transduced with the AAV9-LAH4 complex formed after 0, 30, and 120 min. Total protein was extracted, and western blots were performed using anti-GFP antibody. The Ponceau S-stained total protein was used as a loading control. (D) Quantification of the protein level in (C). Data are means ± SEM (n = 3; one-way ANOVA followed by a t test). **p < 0.01. (E) Effect of incubation temperature on AAV9 transduction efficiency. Scale bar represents 40 μm. (F) Total RNA was isolated from cells incubated at 4°C, 25°C, or 37°C in (E), and mRNA levels of GFP were assessed by quantitative polymerase chain reaction. Data are means ± SEM (n = 3; one-way ANOVA followed by a t test). *p < 0.05, **p < 0.01. (G) GFP protein level in ECs transduced with the AAV9-LAH4 complex formed at 4°C, 25°C, or 37°C. Total protein was extracted and western blots were performed using anti-GFP antibody. The Ponceau S-stained total protein was used as a loading control. (H) Quantification of the protein level in (G). Data are means ± SEM (n = 3; one-way ANOVA followed by t test). *p < 0.05, **p < 0.01.

4°C, there was very weak fluorescence in cells. The fluorescence level significantly increased when the AAV9 vector was incubated with the peptide of LAH4 at 25°C and 37°C. We also extracted the total RNA and protein from the cells in Figure 5E and examined the GFP mRNA level and protein level with quantitative real-time RT-PCR and western blot, respectively. As shown in Figures 5F–5H, similar to the fluorescence level, the LAH4 peptide induced a temperature-dependent increase of GFP mRNA and protein level in ECs. At 37°C, the GFP mRNA and protein level were 220% and 160% higher than those at 4°C, respectively. Taken together, the incubation condition of 37°C for 120 min produced the AAV9-LAH4 complex mixture with the most transduction potency.

LAH4 increased the penetration of AAV9 through the BBB model *in vitro*

It has been reported that AAV9 penetrates brain microvascular EC (BMVEC) barriers more effectively than does AAV2 through an active, cell-mediated process.[38,39] Therefore, we established a BBB model *in vitro*. BMVECs were seeded on cell culture inserts featuring transparent polyethylene terephthalate (PET) membranes with pores, 0.4 μm in diameter. The two-compartment configuration allows for an upper and lower chamber to be separated by polarized BMVECs. AAV9 particles were incubated with phosphate-buffered saline (PBS) or different concentration gradients of LAH4 (20–50 μM), which were then diluted in the media and added to the upper chamber of cell culture inserts. At the indicated time points, media were collected from the lower chambers and analyzed by qPCR for the presence of vector genomes, enabling the monitoring of AAV particles that traffic across the

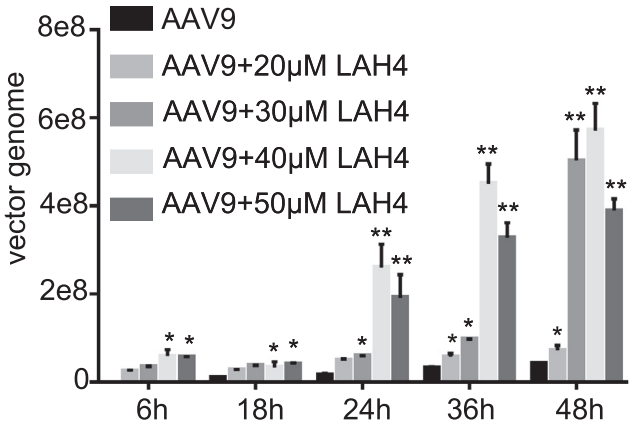

Figure 6. LAH4 increased the penetration of AAV9 through the BBB model *in vitro*

hCMEC/D3 cells were cultured in a monolayer and incubated without or with LAH4 at concentration gradients of 20, 30, 40, and 50 μM. The media in the basal chamber were collected at different time points and the viral titer was analyzed by qPCR. All treatments were performed in triplicate. Data are means ± SEM (n = 3; one-way ANOVA followed by a t test). *p < 0.05, **p < 0.01, compared to cells with the AAV9 treatment.

BMVEC monolayer. As shown in Figure 6, LAH4 significantly increased the penetration of AAV9 through the BBB model, which was reliant on the incubation time of AAV9 with LAH4. We also found that LAH4 could enhance the ability of AAV9 to penetrate the BBB in a dose-dependent manner (20–40 μM). However, LAH4 with a higher concentration (>40 μM) would inhibit the penetration of AAV9 through the BBB.

The LAH4 peptide enhanced the expression of target gene delivered by AAV9 *in vivo*

The BBB is composed of specialized brain microvascular ECs that control the flow of substances into and out of the brain.[36–39] Since CPPs can enhance the transduction of AAV9 vector into ECs, we speculate that CPPs can also enhance transduction of the AAV9 vector in the CNS crossing the BBB. To test this hypothesis, we injected the PBS buffer, AAV9 vector, and AAV9-LAH4 complex mixture into mice intravenously (i.v.). After 3 weeks, the GFP fluorescence in the tissues of liver and brain was examined using the immunohistochemistry method. We selected three different brain regions and one liver region for imaging. As shown in Figures 7A and 7B, there was very weak background fluorescence in both the brain and liver in mice injected with PBS. The fluorescence level in both the brain and liver increased mildly in mice injected with AAV9 vector as expected. In mice injected with the AAV9-LAH4 complex mixture, the number of GFP-expressing cells increased about 250% in hippocampus, 160% in cerebellum, 140% in cortex, and 400% in liver compared to those of mice injected with AAV9 vector only.

To confirm this result, the DNA level and mRNA level of GFP in both the brain and liver were also examined by quantitative real-time RT-PCR. As shown in Figure 7C, the GFP DNA copy numbers in mice injected with the AAV9-LAH4 complex increased about 400% and 580% compared to those in mice injected with AAV9 alone, respectively. Similarly, the GFP mRNA levels in mice injected with the AAV9-LAH4 complex increased about 180% and 500% compared to those in mice injected with AAV9, respectively (Figure 7D). Taken together, the LAH4 peptide enhanced the expression of target gene in the brain and liver delivered by AAV9 through systemic administration *in vivo*.

To confirm that LAH4 can increase the transduction of AAV9 in neurons and other CNS cells, the GFP fluorescence in the tissues of brain was examined by immunohistochemistry using two antibodies, the neuronal nuclear protein (NeuN) antibody and the glial fibrillary acidic protein (GFAP) antibody, which are used to stain mature neurons and numerous cell types of the CNS, including astrocytes and ependymal cells, respectively. As shown in Figures 8A and 8B, there was very weak background GFP fluorescence in cells labeled with anti-NeuN and anti-GFAP antibodies in the brain of mice injected with PBS. Strong GFP fluorescence was found in cells labeled with anti-NeuN and anti-GFAP antibodies in mice injected with AAV9 vector as expected. In mice injected with the AAV9-LAH4 complex mixture, the number of GFP-expressing cells greatly increased compared to those of in mice injected with AAV9 vector only. These results confirm the notion that LAH4 has the potential to increases the ability of AAV9 to cross the BBB and enhance brain transduction, especially in neurons, astrocytes, and ependymal cells.

Immune responses of AAV9 transduction in the brain were reduced by the LAH4 peptide

The systemic administration of AAV usually leads to immune responses, which will reduce the gene therapy efficiency and increase the safety concern of gene therapies. Although we have found that the CPPs can enhance the transduction of AAV9 in the brain, whether the immune responses increased along with the higher transduction in the brain is unknown. To examine the immune response in mice injected with the AAV9-LAH4 complex mixture, we examined the mRNA level of two inflammation factors, interleukin-1β (IL-1β) and tumor necrosis factor-α (TNF-α), by quantitative real-time RT-PCR. As shown in Figure 9A, the mRNA levels of IL-1β and TNF-α in the liver of mice injected with the AAV9-LAH4 complex were about 130% and 140% of those in mice injected with AAV9, respectively, suggesting that the LAH4 peptide increased the immune response in the liver. However, the mRNA levels of IL-1β and TNF-α in the brain of mice injected with AAV9-LAH4 were about 55% and 60% of those in mice injected with AAV9, respectively, suggesting that the LAH4 peptide might have reduced the immune response for AAV9 transduction in the brain. This result was confirmed by the decreased levels of CD4 and CD8 in the brain of the mice injected with AAV9-LAH4 compared to those in mice injected with AAV9 only using the immunohistochemistry method (Figures 9B and 9C). We also found that the CD4 and CD8 levels in the liver of mice transduced with AAV9-LAH4 only mildly increased compared to those in mice transduced with AAV9 only, respectively (Figures S2A and S2B). These data suggest that the

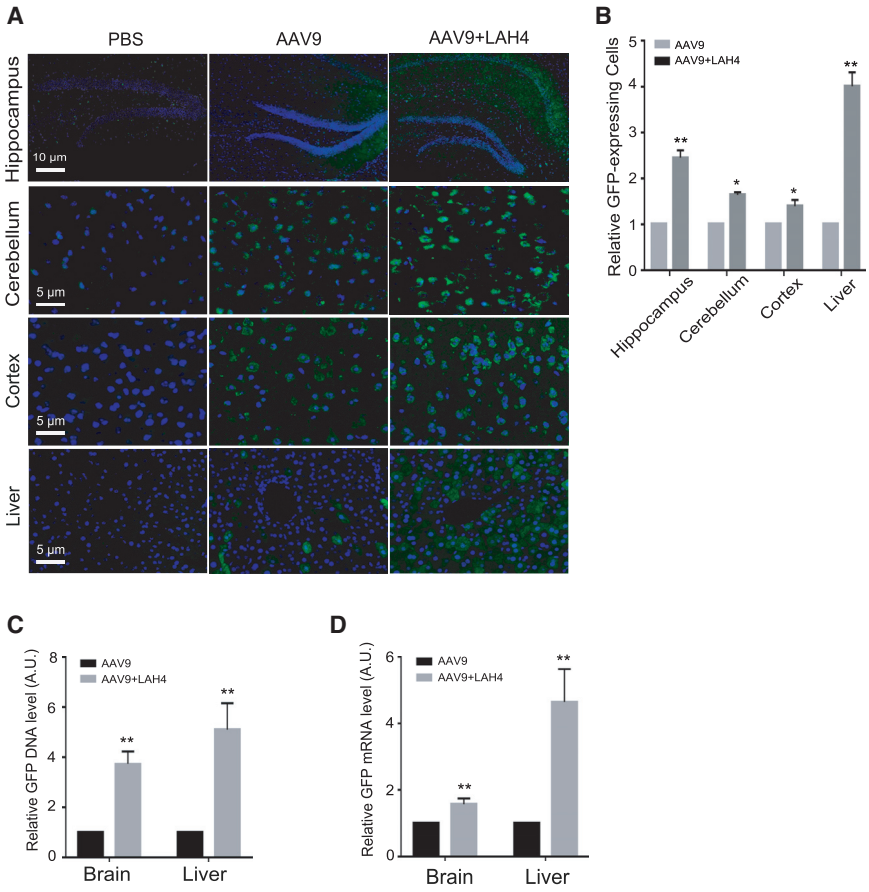

Figure 7. The LAH4 peptide facilitates gene delivery of AAV9 in mouse brain and liver

(A) The transgene expression in tissues from C57BL/6 mice injected with AAV9 or AAV9-LAH4 complexes. Tissues of the liver and brain (hippocampus, cerebellum, cortex) were taken at day 21 after tail vein injection and immunohistochemically stained with antibodies against GFP (green) and liver, respectively. Scale bars represent 5 or 10 μm. (B) Quantification of the relative number of positive cells in (A). Data are means ± SEM (n = 3; one-way ANOVA followed by a t test). *$p < 0.05$, **$p < 0.01$. (C) Genomic DNA was isolated from tissues of the liver and brain and GFP DNA was assessed by qPCR. The $2^{-\Delta\Delta Ct}$ method was used to calculate the relative DNA level. Data are means ± SEM (n = 3; one-way ANOVA followed by a t test). **$p < 0.01$. (D) Total RNA was isolated from tissues of the liver and brain and mRNA levels of GFP were assessed by qPCR. The $2^{-\Delta\Delta Ct}$ method was used to calculate the relative mRNA level. Data are means ± SEM (n = 3; one-way ANOVA followed by a t test). **$p < 0.01$.

LAH4 peptide decreased the immune responses of AAV9 transduction in the brain but not in the liver.

DISCUSSION

Although rAAV vectors are ideal tools for gene therapy and have been widely used for eye diseases, cancers, and vascular diseases, among others,[40–42] their applications for the treatment of CNS diseases have been seriously limited because of their very low efficiency of crossing through the BBB. Several methods have been developed to enhance the capacity of crossing through the BBB and enhance the transduction efficiency for AAV vectors in the CNS, including CPPs. In this study, we found that CPPs can significantly enhance the transduction efficiency of AAV9, the most promising AAV serotype for CNS diseases *in vitro* and *in vivo*.

Efforts have been devoted to improve the transduction efficiency of AAV vectors in the brain. However, very limited progress has been made in this area. Some preclinical studies have shown that engineered AAV vectors have displayed promising results, but further studies suggest that these mutated AAV vectors may not be able to enhance the transduction in large animals and humans. It is also unknown how the mutations on the capsid affect its manufacturing capacity, and whether they lead to any safety concerns are unclear. In addition, AAV engineering is time- and cost-consuming. Therefore, it is necessary to look for an efficient and economic strategy to improve AAV transduction in the CNS. Liu et al.[34] have found that CPPs can efficiently improve the transduction of AAV2 and AAV8 in muscle tissue and no cytotoxicity of CPPs was detected *in vivo*. Zhang et al.[35] found that the THR peptide increased the BBB crossing ability and transduction efficiency in the brain of AAV8 after systemic administration. However, many more AAV8 virions were found in the liver compared to those in the brain (about 175-fold) following systemic administration of the AAV8-THR complex, which is consistent with the previous conclusion that AAV8 is a vector with high liver tropism.[18,43] This result suggests that AAV8 is not an ideal AAV vector to deliver target genes to the brain.[35] In our study, the GFP DNA level in the brain is about 25% of that in the liver of mice transduced with AAV9 vector only (Figure S3), which is consistent with previous reports that AAV9 has relatively high transduction efficiency in the brain compared to other AAV serotypes.[14–16] We also found that the fluorescence level in both the brain and liver in mice transduced with the AAV9-LAH4 complex increased about 1.5- to 4-fols compared to that in mice transduced with AAV9 only (Figures 7A and 7B), suggesting that the LAH4 peptide did not change the tropism of the AAV9 vector and the AAV9-LAH4 complex is an ideal candidate of target gene delivery tool for CNS disease treatment.

One of the main safety concerns for gene therapies using AAV vectors is the immune response, which not only reduces the therapy efficiency but also may cause serious safety issues for patients.[44] Currently, medicines are used to inhibit the immune response when patients are treated with gene therapies.[45] However, because of the BBB barrier, those medicines may not work very well for the immune response

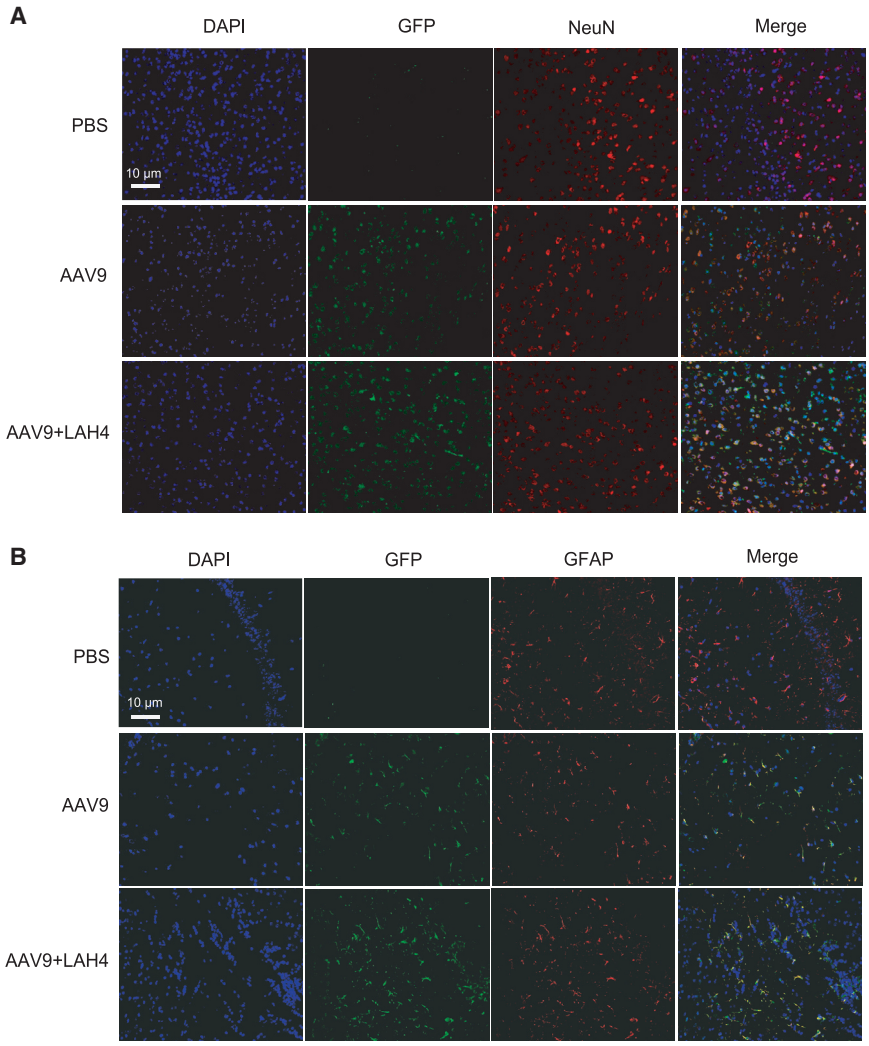

Figure 8. AAV9-LAH4 complex leads to increased transduction in neurons

The transgene expression in neuron cells from C57BL/6 mice injected with PBS, AAV9, or AAV9-LAH4 complexes was examined. (A and B) Tissues of the brain were taken at day 21 day after tail vein injection and immunohistochemically stained with antibodies against GFP (green color) and NeuN (red color) (A) or GFAP (red color) (B), respectively. Representative images of the GFP expression (green) of AAV9, NeuN (red), or GFAP (red) (B) were merged with DAPI (blue). Scale bars represent 10 μm.

induced in the brain. As expected, we found that the mRNA level of two inflammation factors, IL-1β and TNF-α, in the liver of mice transduced with the AAV9-LAH4 complex increased about 30% and 40% compared to those in mice transduced with AAV9 only, respectively. Surprisingly, the mRNA level of IL-1β and TNF-α in the brain of mice transduced with AAV9-LAH4 decreased about 55% and 60% compared to those in mice transduced with AAV9 only, respectively. The reduced immune response by LAH4 in the brain was also confirmed by CD4- and CD8-positive cells using the immunohistochemistry method (Figures 9B and 9C). The different immune responses in the brain and the liver induced by LAH4 are unknown. Further experiments are needed to explore the mechanism of LAH4-induced reduction of immune response in the brain.

As mentioned in this study and previous reports, the enhancement of viral transduction mediated by CPPs is caused by the direct interaction between AAV particles and CPPs. It has been suggested that CPPs can improve the internalization of AAV capsid into cells through the endocytosis process.[34] To explore whether endocytosis also plays a similar role for transduction of the AAV9-LAH4 complex into cells, we examined transduction of the AAV9-LAH4 complex in ECs preincubated with amiloride and chlorpromazine, which are known to block clathrin-mediated internalization and inhibit the macropinocytosis by preventing induction of membrane ruffling, respectively.[46,47] As shown in Figures S4A and S4B, amiloride did not inhibit the transduction of AAV9 in ECs, whereas chlorpromazine did. Both amiloride and chlorpromazine significantly inhibited the transduction efficiency of AAV9-LAH4 into ECs, suggesting that endocytosis plays an important role in this process. The fact that *Erythrina cristagalli* lectin (ECL), which blocks the binding of AAV9 with its receptor,[48] dramatically inhibited the entry of both AAV9 and AAV9-LAH4 into ECs (Figures S4C and S4D), suggesting that the AAV9 receptor also plays an essential role for the entry of AAV9-CPP into cells.

Based on the results in this study, we speculate that the purified AAV-CPP complex may have higher efficiency, better safety, and a lower immune response than those of the unpurified mixture. How to remove unbound impurities in the AAV-CPP complex mixture with high transduction efficiency is a technical challenge that needs to be overcome in the future.

MATERIALS AND METHODS

Cell lines and peptides

HEK293T cells were maintained in Dulbecco's modified Eagle's medium (DMEM) (HyClone, Northbrook, IL, USA) with 10% (v/v) of heat-inactivated fetal bovine serum (FBS) (Sera Pro). The human cerebral microvascular EC (hCMEC) line hCMEC/D3, marked as ECs, was purchased from Sigma-Aldrich (product no. [PN] SCC066). Culture medium contained endothelial basal medium (EBM)-2 (Lonza, Basel, Switzerland) supplemented with 1% lipid concentrate, 1% HEPES, 0.055% cortisol, 0.002% basic fibroblast growth factor (bFGF), and 0.00055% vitamin C. HAs were purchased from Science Cell Research

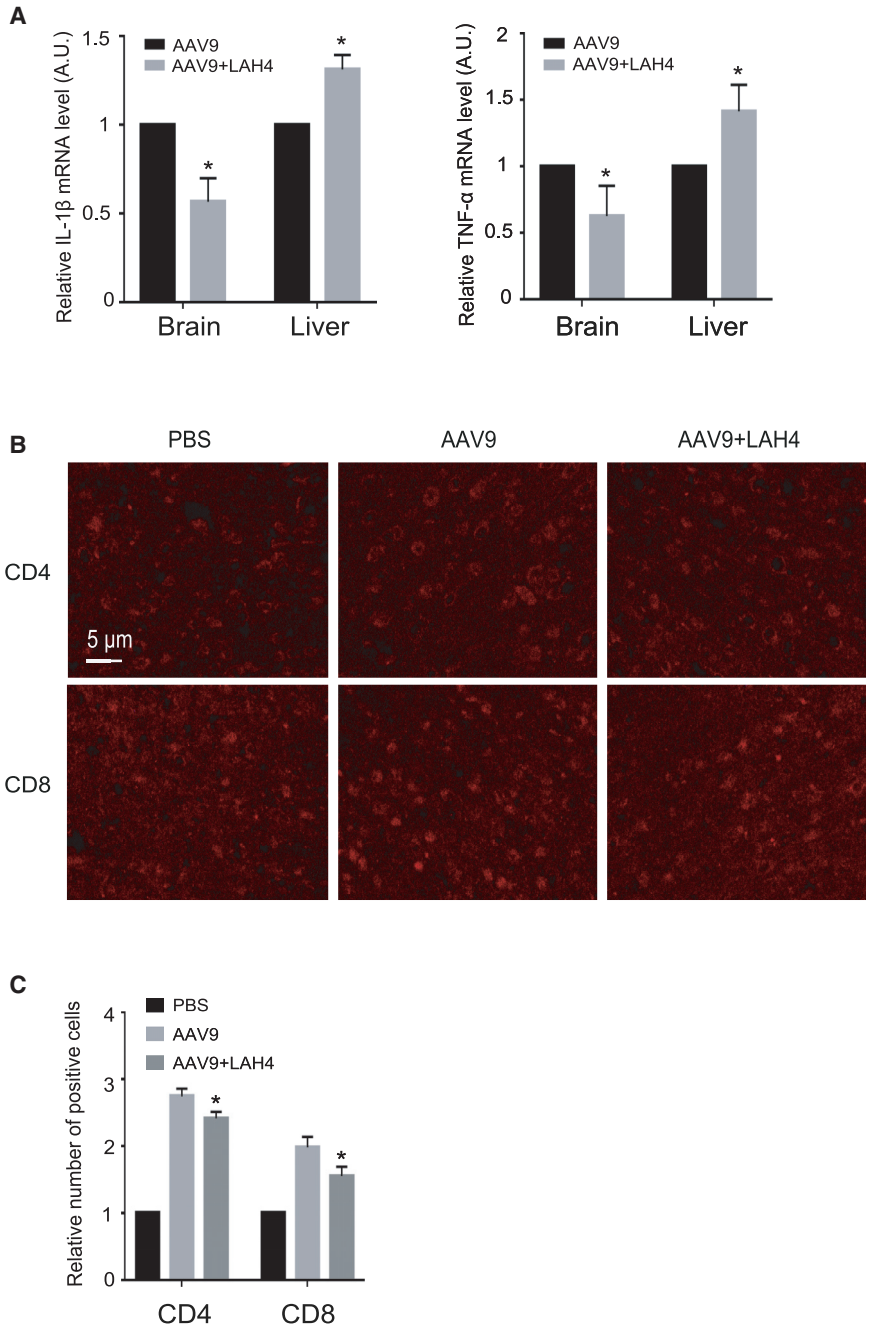

Figure 9. The LAH4 peptide did not increase the immune response in the brain

(A) Total RNA was isolated from tissues of the liver and brain, and mRNA levels of IL-1β and TNF-α were assessed by qPCR. The $2^{-\Delta\Delta Ct}$ method was used to calculate the relative expression of IL-1β and TNF-α. All of the data were then normalized by the mean percentage of cytokine expression in mice injected with AAV9 only. Data are means ± SEM (n = 3; one-way ANOVA followed by a t test). *p < 0.05. (B) Analysis of T lymphocyte infiltration in brain tissues from C57BL/6 mice injected with AAV9 or AAV9-LAH4 complexes at 21 days. Tissues were immunohistochemically stained with antibodies against CD4 and CD8 (red). Scale bar represents 5 μm. (C) Quantification of the relative number of positive cells in (B). Data are means ± SEM (n = 3; one-way ANOVA followed by a t test). *p < 0.05.

Laboratories (Carlsbad, CA, USA) and maintained in astrocyte medium (Science Cell Research Laboratories, Carlsbad, CA, USA). All of the cell lines were cultured in an incubator at the condition of 37°C/5% CO_2. All peptides with >95% purity were synthesized at GenScript (Nanjing, China) and dissolved in Dulbecco's PBS (DPBS) with 10% dimethyl sulfoxide to a stock solution of 10 mM. The amino acid sequences for the peptides of LAH4, ApoE, and Leptin30 are KKALLALALHHLAHLALHLALALKKAC, LRKLRKRLLLRKLRKRLL, and YQQILTSMPSRNVIQISNDLENLRDLLHVL, respectively.

Plasmids

The AAV9 rep/cap plasmid, pAAV/CBA-GFP, and pAD helper plasmid for recombinant AAV9 vector production were obtained from Addgene (Cambridge, MA, USA).

Production of recombinant AAV9 viral vectors

Recombinant AAV9 full particles expressing GFP driven by the chicken β-actin (CBA) promoter were produced using a triple transfection in HEK293T cells as previously described.[49,50] In brief, the transgene plasmid pAAV/CBA-GFP, the AAV helper plasmid containing Rep and Cap genes, and the adenoviral helper plasmid pAD were co-transfected into HEK293T cells. HEK293T cells were collected and lysed 72 h post-transfection. The supernatant was then subjected to a cesium chloride gradient ultracentrifugation.

In vitro transduction assay

At least 6 h before AAV9 transduction, the cells were seeded in 24-well plates with a density of 3×10^5 cells per well. CPPs at different concentrations (final concentration of 0, 5, and 20 μM) were incubated with AAV9/GFP (MOI of 1,000) at 37°C for 2 h. The AAV9 alone or AAV9-peptide complexes were then added to the HEK293T cells, ECs, or HAs. To assess the best temperature for AAV particles and the peptide to interact, AAV-peptide complexes were incubated at 4°C, 25°C, or 37°C, respectively. To explore the optimal incubation time for AAV9 particles and peptides to form AAV-LAH4 complexes with the best transduction efficiency, AAV9-peptide complexes were incubated in time gradients of 0, 1, and 2 h.

Western blot analysis

Total proteins from cells or animal tissues were isolated with radioimmunoprecipitation assay (RIPA) buffer (Beyotime Institute of Biotechnology, Shanghai, China). Protein quantification was performed with a bicinchoninic acid (BCA) protein assay kit (PN WLA004, Wanleibio, Shenyang, China). Equal amounts of protein samples were separated by SDS-PAGE and electrophoretically transferred onto polyvinylidene fluoride (PVDF) membranes. To avoid non-specific binding, membranes were blocked with 5% nonfat milk for 45 min at room temperature. Subsequently, membranes were incubated with anti-GFP antibody (1:100,000 dilution, PN 66002-1-lg, Proteintech, Wuhan, China) for 2 h at room temperature. After washing, the membranes were incubated with horseradish peroxidase (HRP)-conjugated secondary antibodies for 2 h at room temperature (1:5,000 dilution, PN SA00001-1, Proteintech, Wuhan, China). After washing three times with Tris-buffered saline with Tween 20 (TBST), immunoblots were visualized by an enhanced chemiluminescence (ECL) kit (PN 180-5001, Tanon, Shanghai, China) and scanned using the Tanon AllDoc_x. The integrated density values were calculated through ImageJ software.

Real-time PCR assay

The total RNAs were separated from cells and tissues of the brain and liver using TRIzol reagent (PN DP424, TIANGEN, Beijing, China). Then, the concentration and quality of RNA were determined using a NanoPhotometer N50 Touch (Implen). TakaRa PrimeScript RT master mix (RR036A) was used for inverse transcription of total RNA to cDNA. The qPCR was performed on the LightCycler 96 real-time system (Roche) using a pair of primers specific for the GFP transgene, that is, 5′-GCACAAGCTGGAGTACAACTA-3′ (forward) and 5′-TGTTGTGGCGGATCTTGAA-3′ (reverse). Glyceraldehyde 3-phosphate dehydrogenase (GAPDH) was used as the endogenous control. The primers specific for the GAPDH gene are 5′-GAAGGTGAAGGTCGGAGTC-3′ (forward) and 5′-GAAGATG GTGATGGGATTTC-3′ (reverse). The primers specific for the IL-1β gene are 5′-GCAACTGTTCCTGAACTCAAC-3′ (forward) and 5′-ATCTTTTGGGGTCCGTCAACT-3′ (reverse). The primers specific for the TNF-α gene are 5′-CTGAACTTCGGGGTGATCGG-3′ (forward) and 5′-GGCTTGTCACTCGAATTTTGA-3′ (reverse). The genomic DNA (gDNA) was extracted from the tissues using a DNeasy blood & tissue kit (PN DP304, TIANGEN, Beijing, China) and was quantified by qPCR. The relative expression values were calculated using relative quantification ($2^{-\Delta\Delta Ct}$).

Immunofluorescence assays

AAV9 particles and the LAH4-FITC peptide were incubated at 37°C for 1 h. The mixture was then added into cell cultures and incubated for 1 h. After that, ECs and HAs were washed by DPBS buffer three times. The cells were fixed with 4% paraformaldehyde for 20 min and permeabilized with 0.5% Triton X-100 for 40 min at room temperature. After blocking with 5% bovine serum album (BSA) for 30 min, the cells were incubated with AAV primary antibodies (1:10 dilution, PN 65158, Progen) at 4°C overnight. Cells were incubated with DyLight 549-conjugated goat anti-mouse immunoglobulin (Ig)G (1:5,000 dilution, PN 29147, Rockland) for 1 h at room temperature. DAPI (4′,6-diamidino-2-phenylindole) was applied to the samples and incubated for 5 min to visualize cell nuclei. Stained cells were visualized using confocal microscopy (Nikon A1R). To examine the effect of serum on the transduction efficiency of AAV9-LAH4, AAV9 particles and the LAH4-FITC (5 μM) peptide were incubated at 37°C for 1 h. After that, the mouse serum was added into the mixture to final concentrations of 10%, 20%, and 30% (v/v) and incubated for another 2 h. The mixtures with serum were then added into EC cultures and incubated for 1 h for the transduction assay.

In vitro internalization and intracellular trafficking study

The ECs were preincubated without or with amiloride (1 mmol/L) or chlorpromazine (15 μg/mL) for 30 min at 37°C. Then, the cells were infected with the AAV9 vector or the AAV9-LAH4 complex. The cells were also treated with ECL (50 μg/mL) for 15 min at 4°C. The cells were then washed and AAV9 or AAV9-LAH4 complexes were added into the solution and incubated at 4°C for 1 h. GFP expression was analyzed by western blot 2 days after infection.

In vitro BBB model and transcytosis assays

hCMEC/D3 cells were seeded into positron-emission tomography (PET) track-etched membranes (0.4-μm pores) and a 24-well transwell plate, which were both coated with rat-tail collagen type I and rinsed with 1× PBS. The hCMEC/D3 cells at a density of 5×10^4 cells/insert and the medium were changed every 2 days. After about 1 week, an electric cell-substrate impedance system (MERS00002) was used detected transendothelial electrical resistance (TEER) readings. When the reading was stable at 1,000 Ω, cells were washed with DPBS and cultured in serum-free medium. AAV9 or AAV9-LAH4 (20–50 μM) vectors were applied to the upper chamber at 2×10^9 vg. Cultures were then incubated with the virus at 37°C with 5% CO_2. The culture medium of the lower chamber was collected at the designated time point at 6, 18, 24, 36, and 48 h. Viral titers were calculated by qPCR.

Animal study

C57BL/6 female mice at 5 weeks of age were purchased from the Weitonglihua (Beijing, China). All mice were randomly divided into groups of three animals each and maintained in a specific pathogen-free facility at China Medical University. Mice were administered either AAV9/GFP or an AAV9/GFP-peptides complex via tail vein injection. After 3 weeks of injection, mice were euthanized, and the tissues were collected. All procedures were approved by the China Medical University Animal Ethics Committee and conducted in accordance with China Animal Welfare and Biosecurity Legislation.

Immunohistochemistry assays

AAV9 (3×10^{11} particles/mouse) was pre-incubated with 0.001 mmol LAH4 peptide for 2 h at 37°C. The AAV9 or AAV9-CPP complexes were injected via tail vein into C57BL/6 mice. After 21 days of injection, the brain and liver of mice were excised, fixed,

frozen, cryosectioned, and then mounted onto glass slides (Thermo Scientific, Cryotome E). Frozen sections were then washed with cold PBS. After fixation with 4% paraformaldehyde in antigen retrieval buffer (100× EDTA buffer, pH 8.0), the slides were blocked with 3% BSA and then washed by PBS, followed by incubation with rabbit anti-GFP (Proteintech PN 50430-2-AP), rat anti-CD4 (Abs120100), or anti-CD8 (Abs120101). After that, the slides were incubated with secondary antibody, and then counterstained with DAPI for 10 min (KeyGEN BioTECH PN KGA215). Fluorescence images were acquired by Nikon DS-U3 controller using a Nikon Eclipse C1 microscope. Regions of interest were randomly chosen per image at ×200 magnification.

Statistical analysis

The results are expressed as means ± SEM (standard error of the mean). The significance of the difference in the means was determined by a Student's t test.

SUPPLEMENTAL INFORMATION

Supplemental information can be found online at https://doi.org/10.1016/j.omtm.2021.02.019.

ACKNOWLEDGMENTS

We thank Drs. Difei Wang and Shengnan Meng for helpful suggestions. This work was supported by the Department of Science and Technology of Liaoning (no. 2018416018).

AUTHOR CONTRIBUTIONS

Y.M., D.S., Y.L., and G.L. designed research; Y.M., D.S., Y.Q., and X.D. performed research; Y.M., D.S., Y.Q., Y.L., and G.L. analyzed data; and Y.M., D.S., Y.L., and G.L. wrote the paper.

DECLARATION OF INTERESTS

The authors declare no competing interests.

REFERENCES

1. Berns, K.I., and Muzyczka, N. (2017). AAV: an overview of unanswered questions. Hum. Gene Ther. *28*, 308–313.
2. Wang, D., Tai, P.W.L., and Gao, G. (2019). Adeno-associated virus vector as a platform for gene therapy delivery. Nat. Rev. Drug Discov. *18*, 358–378.
3. Gaudet, D., Méthot, J., Déry, S., Brisson, D., Essiembre, C., Tremblay, G., Tremblay, K., de Wal, J., Twisk, J., van den Bulk, N., et al. (2013). Efficacy and long-term safety of alipogene tiparvovec (AAV1-LPLS447X) gene therapy for lipoprotein lipase deficiency: an open-label trial. Gene Ther. *20*, 361–369.
4. Mingozzi, F., and High, K.A. (2011). Therapeutic in vivo gene transfer for genetic disease using AAV: progress and challenges. Nat. Rev. Genet. *12*, 341–355.
5. Büning, H. (2013). Gene therapy enters the pharma market: the short story of a long journey. EMBO Mol. Med. *5*, 1–3.
6. Hoy, S.M. (2019). Onasemnogene abeparvovec: first global approval. Drugs *79*, 1255–1262.
7. Bors, L., and Erdő, F. (2019). Overcoming the blood-brain barrier. challenges and tricks for CNS drug delivery. Sci. Pharm. *87*, 6.
8. Hanlon, K.S., Meltzer, J.C., Buzhdygan, T., Cheng, M.J., Sena-Esteves, M., Bennett, R.E., Sullivan, T.P., Razmpour, R., Gong, Y., Ng, C., et al. (2019). Selection of an efficient AAV vector for robust CNS transgene expression. Mol. Ther. Methods Clin. Dev. *15*, 320–332.
9. Johnson, T.B., White, K.A., Brudvig, J.J., Cain, J.T., Langin, L., Pratt, M.A., Booth, C.D., Timm, D.J., Davis, S.S., Meyerink, B., et al. (2021). AAV9 gene therapy increases lifespan and treats pathological and behavioral abnormalities in a mouse model of CLN8-batten disease. Mol. Ther. *29*, 162–175.
10. Saberi, S., Stauffer, J.E., Schulte, D.J., and Ravits, J. (2015). Neuropathology of amyotrophic lateral sclerosis and its variants. Neurol. Clin. *33*, 855–876.
11. Lyon, M.S., Wosiski-Kuhn, M., Gillespie, R., Caress, J., and Milligan, C. (2019). Inflammation, Immunity, and amyotrophic lateral sclerosis: I. Etiology and pathology. Muscle Nerve *59*, 10–22.
12. Choudhury, S.R., Fitzpatrick, Z., Harris, A.F., Maitland, S.A., Ferreira, J.S., Zhang, Y., Ma, S., Sharma, R.B., Gray-Edwards, H.L., Johnson, J.A., et al. (2016). In vivo selection yields AAV-B1 capsid for central nervous system and muscle gene therapy. Mol. Ther. *24*, 1247–1257.
13. Choudhury, S.R., Harris, A.F., Cabral, D.J., Keeler, A.M., Sapp, E., Ferreira, J.S., Gray-Edwards, H.L., Johnson, J.A., Johnson, A.K., Su, Q., et al. (2016). Widespread central nervous system gene transfer and silencing after systemic delivery of novel AAV-AS vector. Mol. Ther. *24*, 726–735.
14. Manfredsson, F.P., Rising, A.C., and Mandel, R.J. (2009). AAV9: a potential blood-brain barrier buster. Mol. Ther. *17*, 403–405.
15. Saunders, N.R., Joakim, E.C., and Dziegielewska, K.M. (2009). The neonatal blood-brain barrier is functionally effective, and immaturity does not explain differential targeting of AAV9. Nat. Biotechnol. *27*, 804–805.
16. Aschauer, D.F., Kreuz, S., and Rumpel, S. (2013). Analysis of transduction efficiency, tropism and axonal transport of AAV serotypes 1, 2, 5, 6, 8 and 9 in the mouse brain. PLoS ONE *8*, e76310.
17. Hammond, S.L., Leek, A.N., Richman, E.H., and Tjalkens, R.B. (2017). Cellular selectivity of AAV serotypes for gene delivery in neurons and astrocytes by neonatal intracerebroventricular injection. PLoS ONE *12*, e0188830.
18. Sands, M.S. (2012). AAV-mediated liver-directed gene therapy. Methods Mol. Biol. *807*, 141–157.
19. Duan, D. (2016). Systemic delivery of adeno-associated viral vectors. Curr. Opin. Virol. *21*, 16–25.
20. Saraiva, J., Nobre, R.J., and Pereira de Almeida, L. (2016). Gene therapy for the CNS using AAVs: the impact of systemic delivery by AAV9. J. Control. Release *241*, 94–109.
21. Barnes, C., Scheideler, O., and Schaffer, D. (2019). Engineering the AAV capsid to evade immune responses. Curr. Opin. Biotechnol. *60*, 99–103.
22. Rabinowitz, J., Chan, Y.K., and Samulski, R.J. (2019). Adeno-associated virus (AAV) versus immune response. Viruses *11*, 102.
23. Mingozzi, F., and High, K.A. (2013). Immune responses to AAV vectors: overcoming barriers to successful gene therapy. Blood *122*, 23–36.
24. Jackson, K.L., Dayton, R.D., Deverman, B.E., and Klein, R.L. (2016). Better targeting, better efficiency for wide-scale neuronal transduction with the synapsin promoter and AAV-PHP.B. Front. Mol. Neurosci. *9*, 116.
25. Liguore, W.A., Domire, J.S., Button, D., Wang, Y., Dufour, B.D., Srinivasan, S., and McBride, J.L. (2019). AAV-PHP.B administration results in a differential pattern of CNS biodistribution in non-human primates compared with mice. Mol. Ther. *27*, 2018–2037.
26. Matsuzaki, Y., Tanaka, M., Hakoda, S., Masuda, T., Miyata, R., Konno, A., and Hirai, H. (2019). Neurotropic properties of AAV-PHP.B are shared among diverse inbred strains of mice. Mol. Ther. *27*, 700–704.
27. Hordeaux, J., Wang, Q., Katz, N., Buza, E.L., Bell, P., and Wilson, J.M. (2018). The neurotropic properties of AAV-PHP.B are limited to C57BL/6J mice. Mol. Ther. *26*, 664–668.
28. Chan, K.Y., Jang, M.J., Yoo, B.B., Greenbaum, A., Ravi, N., Wu, W.L., Sánchez-Guardado, L., Lois, C., Mazmanian, S.K., Deverman, B.E., and Gradinaru, V. (2017). Engineered AAVs for efficient noninvasive gene delivery to the central and peripheral nervous systems. Nat. Neurosci. *20*, 1172–1179.
29. Stalmans, S., Bracke, N., Wynendaele, E., Gevaert, B., Peremans, K., Burvenich, C., Polis, I., and De Spiegeleer, B. (2015). Cell-penetrating peptides selectively cross the blood-brain barrier in vivo. PLoS ONE *10*, e0139652.

30. Zahid, M., and Robbins, P.D. (2015). Cell-type specific penetrating peptides: therapeutic promises and challenges. Molecules *20*, 13055–13070.

31. Silva, S., Almeida, A.J., and Vale, N. (2019). Combination of cell-penetrating peptides with nanoparticles for therapeutic application: a review. Biomolecules *9*, 22.

32. Guidotti, G., Brambilla, L., and Rossi, D. (2017). Cell-penetrating peptides: from basic research to clinics. Trends Pharmacol. Sci. *38*, 406–424.

33. Bechara, C., and Sagan, S. (2013). Cell-penetrating peptides: 20 years later, where do we stand? FEBS Lett. *587*, 1693–1702.

34. Liu, Y., Kim, Y.J., Ji, M., Fang, J., Siriwon, N., Zhang, L.I., and Wang, P. (2014). Enhancing gene delivery of adeno-associated viruses by cell-permeable peptides. Mol. Ther. Methods Clin. Dev. *1*, 12.

35. Zhang, X., He, T., Chai, Z., Samulski, R.J., and Li, C. (2018). Blood-brain barrier shuttle peptides enhance AAV transduction in the brain after systemic administration. Biomaterials *176*, 71–83.

36. Pulgar, V.M. (2019). Transcytosis to cross the blood brain barrier, new advancements and challenges. Front. Neurosci. *12*, 1019.

37. Ayloo, S., and Gu, C. (2019). Transcytosis at the blood-brain barrier. Curr. Opin. Neurobiol. *57*, 32–38.

38. Körbelin, J., Dogbevia, G., Michelfelder, S., Ridder, D.A., Hunger, A., Wenzel, J., Seismann, H., Lampe, M., Bannach, J., Pasparakis, M., et al. (2016). A brain microvasculature endothelial cell-specific viral vector with the potential to treat neurovascular and neurological diseases. EMBO Mol. Med. *8*, 609–625.

39. Di Pasquale, G., and Chiorini, J.A. (2006). AAV transcytosis through barrier epithelia and endothelium. Mol. Ther. *13*, 506–516.

40. Nienhuis, A.W., Nathwani, A.C., and Davidoff, A.M. (2017). Gene therapy for hemophilia. Mol. Ther. *25*, 1163–1167.

41. Rahim, A.A., Wong, A.M.S., Hoefer, K., Buckley, S.M.K., Mattar, C.N., Cheng, S.H., Chan, J.K.Y., Cooper, J.D., and Waddington, S.N. (2011). Intravenous administration of AAV2/9 to the fetal and neonatal mouse leads to differential targeting of CNS cell types and extensive transduction of the nervous system. FASEB J. *25*, 3505–3518.

42. Santiago-Ortiz, J.L., and Schaffer, D.V. (2016). Adeno-associated virus (AAV) vectors in cancer gene therapy. J. Control. Release *240*, 287–301.

43. Sen, D., Gadkari, R.A., Sudha, G., Gabriel, N., Kumar, Y.S., Selot, R., Samuel, R., Rajalingam, S., Ramya, V., Nair, S.C., et al. (2013). Targeted modifications in adeno-associated virus serotype 8 capsid improves its hepatic gene transfer efficiency in vivo. Hum. Gene Ther. Methods *24*, 104–116.

44. Colella, P., Ronzitti, G., and Mingozzi, F. (2017). Emerging issues in AAV-mediated *in vivo* gene therapy. Mol. Ther. Methods Clin. Dev. *8*, 87–104.

45. Chai, Z., Zhang, X., Dobbins, A.L., Rigsbee, K.M., Wang, B., Samulski, R.J., and Li, C. (2019). Optimization of dexamethasone administration for maintaining global transduction efficacy of adeno-associated virus serotype 9. Hum. Gene Ther. *30*, 829–840.

46. West, M.A., Bretscher, M.S., and Watts, C. (1989). Distinct endocytotic pathways in epidermal growth factor-stimulated human carcinoma A431 cells. J. Cell Biol. *109*, 2731–2739.

47. Wang, L.H., Rothberg, K.G., and Anderson, R.G. (1993). Mis-assembly of clathrin lattices on endosomes reveals a regulatory switch for coated pit formation. J. Cell Biol. *123*, 1107–1117.

48. Bell, C.L., Vandenberghe, L.H., Bell, P., Limberis, M.P., Gao, G.P., Van Vliet, K., Agbandje-McKenna, M., and Wilson, J.M. (2011). The AAV9 receptor and its modification to improve in vivo lung gene transfer in mice. J. Clin. Invest. *121*, 2427–2435.

49. Kohlbrenner, E., and Weber, T. (2017). Production and characterization of vectors based on the cardiotropic AAV serotype 9. Methods Mol. Biol. *1521*, 91–107.

50. Ayuso, E., Mingozzi, F., Montane, J., Leon, X., Anguela, X.M., Haurigot, V., Edmonson, S.A., Africa, L., Zhou, S., High, K.A., et al. (2010). High AAV vector purity results in serotype- and tissue-independent enhancement of transduction efficiency. Gene Ther. *17*, 503–510.